

Mueller-Navelet jets

Grigorios Chachamis & Agustín Sabio Vera

GC: Laboratory of Instrumentation and Experimental Particle Physics, Lisbon
ASV: Universidad Autónoma de Madrid, Instituto de Física Teórica UAM/CSIC



EF06 Hadronic Structure & Forward QCD,
Snowmass 2021, July 15th, 2020

- 1 Multi-Regge limit [6]
- 2 Monte Carlo event generator BFKLex [6]
- 3 Collinear double logs [9]
- 4 Odderon & high energy complexity [13]

- 1 Multi-Regge limit [6]
- 2 Monte Carlo event generator BFKLex [6]
- 3 Collinear double logs [9]
- 4 Odderon & high energy complexity [13]

Regge theory preludes QCD. Pomeron in terms of quarks & gluons?

Perturbation theory with large scale $Q > \Lambda_{\text{QCD}} \rightarrow \alpha_s(Q) \ll 1$.

$s \gg t, Q^2 \rightarrow \alpha_s(Q) \log\left(\frac{s}{t}\right) \sim \mathcal{O}(1)$. Resummation needed.

$$\sigma_{\text{tot}}(s = e^{y_A - y_B}) = \sum_{n=0}^{\infty} \left| \begin{array}{c} \text{Diagram} \end{array} \right| \cdot \frac{1}{s}$$

$s \rightarrow \infty$ $n=0$ $y_A \gg y_1 \gg \dots \gg y_n \gg y_B$

MULTI-REGGE
KINEMATICS

$$\sigma_{\text{tot}}^{\text{LL}} = \sum_{n=0}^{\infty} C_n^{\text{LL}} \alpha_s^n \int_{y_B}^{y_A} dy_1 \int_{y_B}^{y_1} dy_2 \cdots \int_{y_B}^{y_{n-1}} dy_n = \sum_{n=0}^{\infty} \frac{C_n^{\text{LL}}}{n!} \underbrace{\alpha_s^n (y_A - y_B)^n}_{\text{LL}}$$

Multi-particle production linked to elastic amplitudes via optical theorem:

$$\sigma_{\text{tot}}(s = e^{y_A - y_B}) = \sum_{n=0}^{\infty} \left| \text{Diagram} \right|^2 \cdot \frac{1}{s} = \frac{1}{s} \sum_{n=0}^{\infty} \left| \text{Diagram} \right|^2 = \frac{1}{s} \text{Im} A_{\text{elast}}(s, t=0)$$

$s \rightarrow \infty$
 $y_A \gg y_1 \gg \dots \gg y_n \gg y_B$
 MULTI-REGGE
 PROCESS DEPENDENT
 UNIVERSAL
 PROCESS DEPENDENT
 HARD POMERON

$$A_{\text{elast}}(s, t) = \sum_{n=0}^{\infty} \left| \text{Diagram} \right|^2$$

PROCESS DEPENDENT
 UNIVERSAL
 PROCESS DEPENDENT
 HARD POMERON

New degree of freedom
= Reggeized gluon

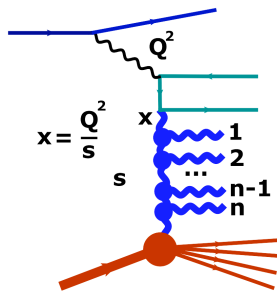
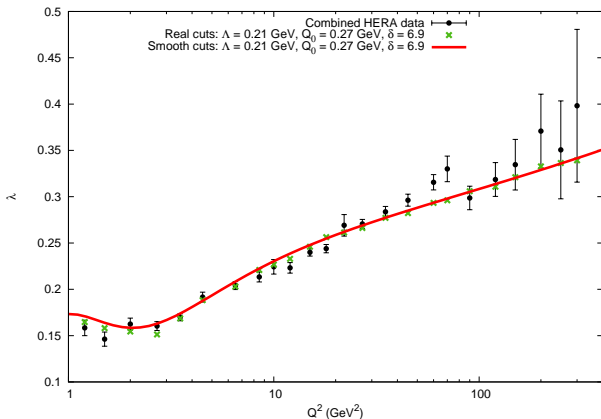
Pomeron = Composite state

2-dim interaction Hamiltonian

Important Bootstrap relations

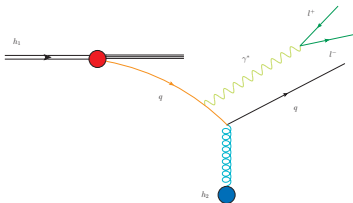
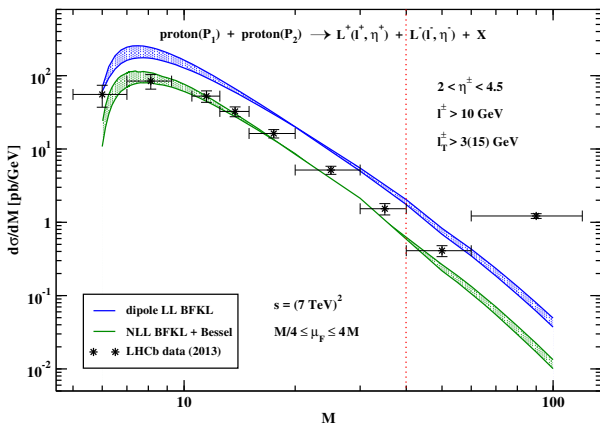
DIS data: $F_2(x, Q^2) \simeq x^{-\lambda(Q^2)}$

A NLL Multi-Regge approach fits data well (Hentschinski-Salas-SV)²⁰¹²



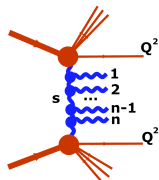
Transition from a perturbative to a non-perturbative Pomeron not well understood. Need more exclusive observables: LHC is the playground now.

Forward Drell-Yan production at LHC (Celiberto-Gordo-SV)²⁰¹⁸
 The same unintegrated gluon density works well for current data



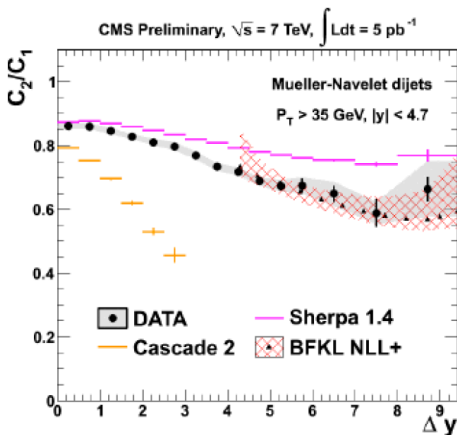
Previous analysis by (Brzeminski-Motyka-Sadzikowski-Stebel)
 We work with BFKL at NLL plus collinear corrections

LHC observable proposed as ideal to pin down original BFKL, without collinear contamination: remove χ_0



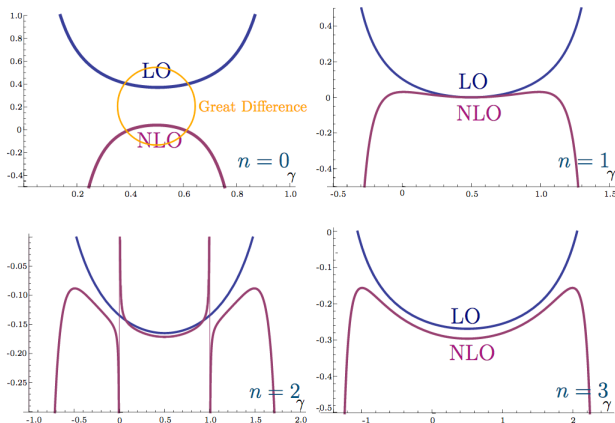
(Del Duca-Stirling)^{Tevatron}
 $\langle \cos(m\theta) \rangle \simeq e^{\alpha Y(\chi_m - \chi_0)}$

(SV)²⁰⁰⁶ (SV-Schwennsen)²⁰⁰⁷
 $\mathcal{R}_{m,n} = \frac{\langle \cos(m\theta) \rangle}{\langle \cos(n\theta) \rangle}$
 $\simeq e^{\alpha Y(\chi_m - \chi_n)}$



Confirmed in 2013 (Wallon et al) (Colferai et al) (Papa et al)

Why? $n > 0$ stable under radiative corrections
 $n = 0$ only one sensitive to collinear radiation



Plots for $\alpha\chi_n^{(LO)}(\gamma) + \alpha^2\chi_n^{(NLO)}(\gamma) + \text{Collinear corrections}$

- 1 Multi-Regge limit [6]
- 2 Monte Carlo event generator BFKLex [6]
- 3 Collinear double logs [9]
- 4 Odderon & high energy complexity [13]

Effective Feynman rules: basis of Lipatov's High Energy effective action

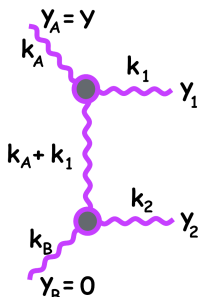
Gluon Regge trajectory: $\omega(\vec{q}) = -\frac{\alpha_s N_c}{\pi} \log \frac{q^2}{\lambda^2}$

Non-IR finite

Modified propagators in the t -channel:

$$\left(\frac{s_i}{s_0}\right)^{\omega(t_i)} = e^{\omega(t_i)(y_i - y_{i+1})}$$

$$\left(\frac{\alpha_s N_c}{\pi}\right)^2 \int d^2 \vec{k}_1 \frac{\theta(k_1^2 - \lambda^2)}{\pi k_1^2} \int d^2 \vec{k}_2 \frac{\theta(k_2^2 - \lambda^2)}{\pi k_2^2} \delta^{(2)}(\vec{k}_A + \vec{k}_1 + \vec{k}_2 - \vec{k}_B) \\ \times \int_0^Y dy_1 \int_0^{y_1} dy_2 e^{\omega(\vec{k}_A)(Y - y_1)} e^{\omega(\vec{k}_A + \vec{k}_1)(y_1 - y_2)} e^{\omega(\vec{k}_A + \vec{k}_1 + \vec{k}_2)y_2}$$



Each diagram is Non-IR finite when $\lambda \rightarrow 0$.

Only after summation over all possible final states we get IR finiteness

$$\sigma(Q_1, Q_2, Y) = \int d^2\vec{k}_A d^2\vec{k}_B \underbrace{\phi_A(Q_1, \vec{k}_A) \phi_B(Q_2, \vec{k}_B)}_{\text{PROCESS-DEPENDENT}} \underbrace{f(\vec{k}_A, \vec{k}_B, Y)}_{\text{UNIVERSAL}}$$

$$f(\vec{k}_A, \vec{k}_B, Y) = \sum_n \left| \begin{array}{c} \gamma_A = Y, k_A \\ \vdots \\ \gamma_1, k_1 \\ \gamma_2, k_2 \\ \vdots \\ \gamma_n, k_n \\ \vdots \\ \gamma_B = 0, k_B \end{array} \right|^2$$

$$= e^{\omega(\vec{k}_A)Y} \left\{ \delta^{(2)}(\vec{k}_A - \vec{k}_B) + \sum_{n=1}^{\infty} \prod_{i=1}^n \frac{\alpha_s N_c}{\pi} \int d^2\vec{k}_i \frac{\theta(k_i^2 - \lambda^2)}{\pi k_i^2} \right.$$

$$\left. \times \int_0^{y_i-1} dy_i e^{(\omega(\vec{k}_A + \sum_{l=1}^i \vec{k}_l) - \omega(\vec{k}_A + \sum_{l=1}^{i-1} \vec{k}_l))y_i} \delta^{(2)}\left(\vec{k}_A + \sum_{l=1}^n \vec{k}_l - \vec{k}_B\right) \right\}$$

BFKLex: Monte Carlo implementation of full NLL BFKL

NLL is more complicated, sensitive to the running & choice of energy scale:

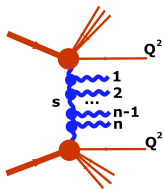
$$\begin{aligned}\sigma_{\text{tot}}^{\text{NLL}} &= \sum_{n=1}^{\infty} \frac{C_n^{\text{LL}}(\mathbf{k}_i)}{n!} (\alpha_s - \mathcal{A}\alpha_s^2)^n (y_A - y_B - \mathcal{B})^n \\ &= \sigma_{\text{tot}}^{\text{LL}} - \sum_{n=1}^{\infty} \frac{(\mathcal{B} C_n^{\text{LL}}(\mathbf{k}_i) + (n-1)\mathcal{A} C_{n-1}^{\text{LL}}(\mathbf{k}_i))}{(n-1)!} \underbrace{\alpha_s^n (y_A - y_B)^{n-1}}_{\text{NLL}}\end{aligned}$$

besides, quarks enter the game ...

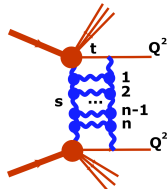
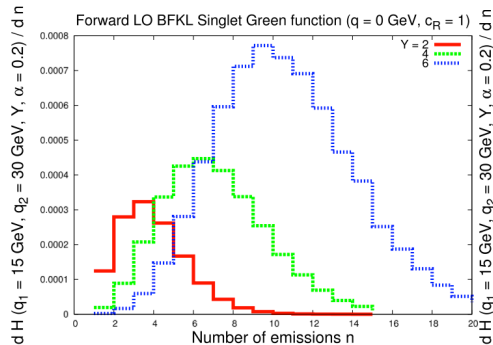
All of this is captured by Quasi-Multi-Regge kinematics.

Important Bootstrap relations also at NLL

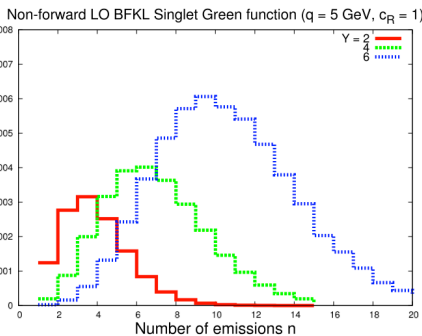
 (Fadin et al)



Cut Pomeron: Number of emissions?

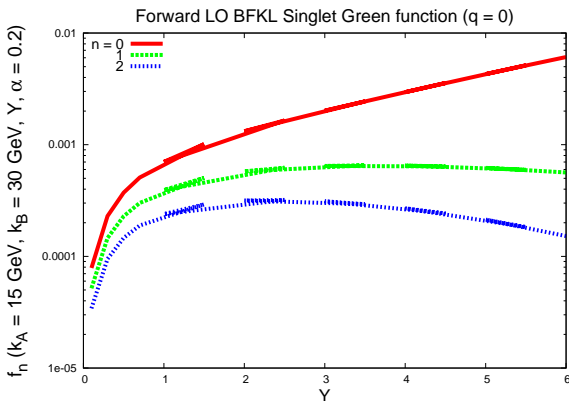


Pomeron: Number of rungs?



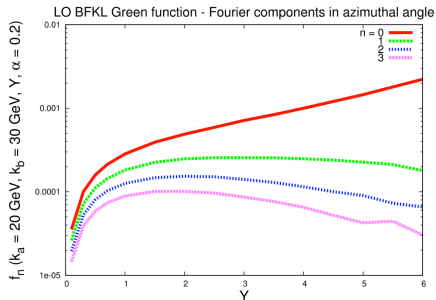
Growth with energy? Depends on the azimuthal angle Fourier component:

$$f_n \left(|\vec{k}_A|, |\vec{k}_B|, Y \right) = \int_0^{2\pi} \frac{d\theta}{2\pi} f \left(\vec{k}_A, \vec{k}_B, Y \right) \cos(n\theta)$$

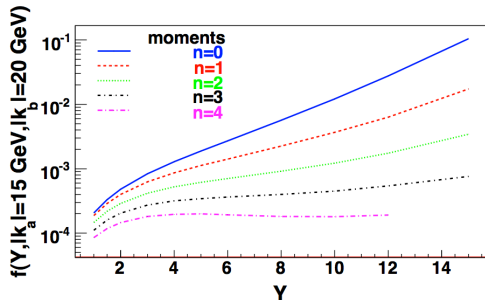


This is a distinct feature of BFKL

BFKL



CCFM



All (Catani-Ciafaloni-Fiorani-Marchesini) projections grow with energy,
 not in BFKL (GC-Stephens-SV)²⁰¹¹

Observables only sensitive to $n > 0$
 single out original BFKL

- 1 Multi-Regge limit [6]
- 2 Monte Carlo event generator BFKLex [6]
- 3 Collinear double logs [9]
- 4 Odderon & high energy complexity [13]

We can extend the formalism to include collinear regions

$$f = e^{\omega(\vec{k}_A)Y} \left\{ \delta^{(2)}(\vec{k}_A - \vec{k}_B) + \sum_{n=1}^{\infty} \prod_{i=1}^n \frac{\alpha_s N_c}{\pi} \int d^2\vec{k}_i \frac{\theta(k_i^2 - \lambda^2)}{\pi k_i^2} \right. \\ \left. \times \int_0^{y_i-1} dy_i e^{(\omega(\vec{k}_A + \sum_{l=1}^i \vec{k}_l) - \omega(\vec{k}_A + \sum_{l=1}^{i-1} \vec{k}_l))y_i} \delta^{(2)}\left(\vec{k}_A + \sum_{l=1}^n \vec{k}_l - \vec{k}_B\right) \right\}$$

Key at NLL:

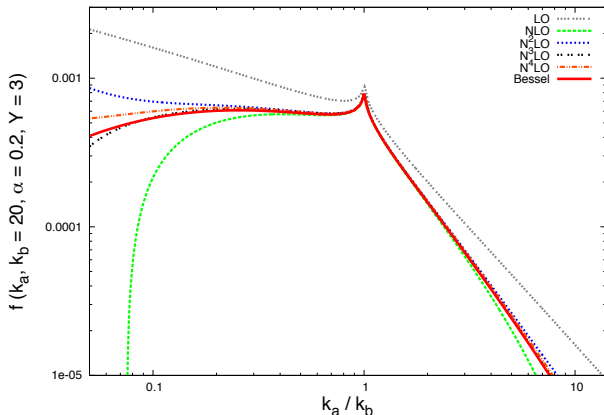
$$\theta(k_i^2 - \lambda^2) \rightarrow \theta(k_i^2 - \lambda^2) - \underbrace{\frac{\bar{\alpha}_s}{4} \ln^2 \left(\frac{\vec{k}_A^2}{(\vec{k}_A + \vec{k}_i)^2} \right)}_{\text{NLL}}$$

Resum it to all orders (SV)²⁰⁰⁵:

$$\theta(k_i^2 - \lambda^2) \rightarrow \theta(k_i^2 - \lambda^2) + \sum_{n=1}^{\infty} \frac{(-\bar{\alpha}_s)^n}{2^n n! (n+1)!} \ln^{2n} \left(\frac{\vec{k}_A^2}{(\vec{k}_A + \vec{k}_i)^2} \right)$$

It corresponds to a Bessel function $J_1 \left(\sqrt{2\bar{\alpha}_s \ln^2 \left(\frac{\vec{k}_A^2}{(\vec{k}_A + \vec{k}_i)^2} \right)} \right)$

$$\sigma(Q_1, Q_2, Y) = \int d^2\mathbf{k}_a d^2\mathbf{k}_b \phi_A(Q_1, \mathbf{k}_a) \phi_B(Q_2, \mathbf{k}_b) f(\mathbf{k}_a, \mathbf{k}_b, Y)$$

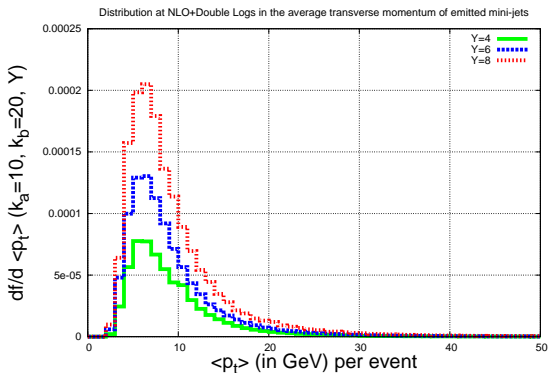
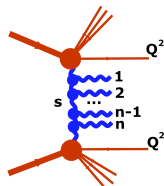


Important to go beyond the MRK limit (Ciafaloni-Colferai-Salam-Stasto).
For original BFKL we need “ δ -like” impact factors $\phi_{A,B}$ & $Q_1 \simeq Q_2$.

Implementation in BFKLex

Average transverse momentum of emitted mini-jets?

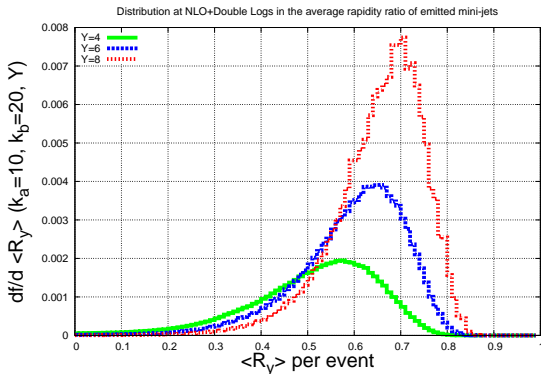
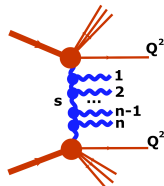
$$\langle p_t \rangle = \frac{1}{n} \sum_{i=1}^n |k_i|$$



Mini-jet $\langle p_t \rangle_{\max}$ independent of rapidity separation of tagged forward jets.

Average rapidity separation among emitted mini-jets?

$$\langle \mathcal{R}_y \rangle = \frac{1}{n+1} \sum_{i=1}^{n+1} \frac{y_i}{y_{i-1}} \simeq 1 + \frac{\Delta}{Y} \ln \frac{\Delta}{Y}$$

if $Y \simeq N\Delta$ in MRK and $Y \gg \Delta$ 

Higher $\langle \mathcal{R}_y \rangle_{\max}$ for higher energies: $\Delta_{\text{LO}} \simeq 0.62$, $\Delta_{\text{LO+DLs}} \simeq 0.81$
 Lower mini-jet multiplicity when including higher order corrections

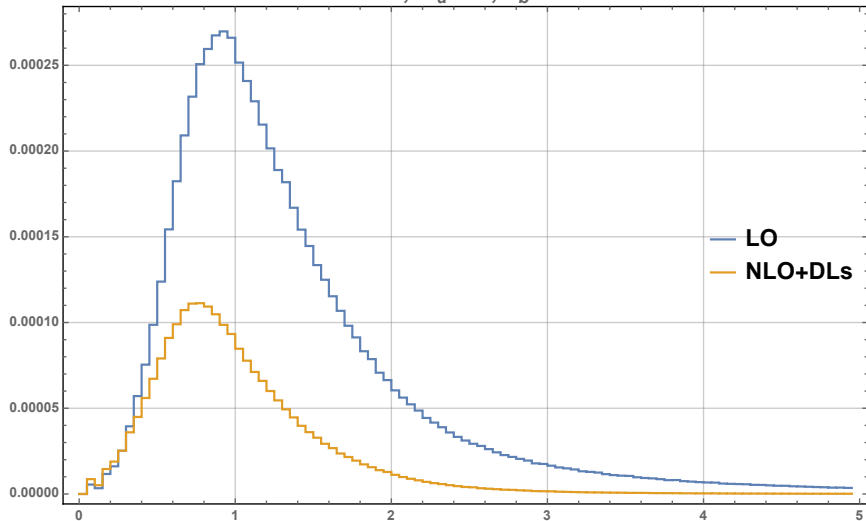
A new observable

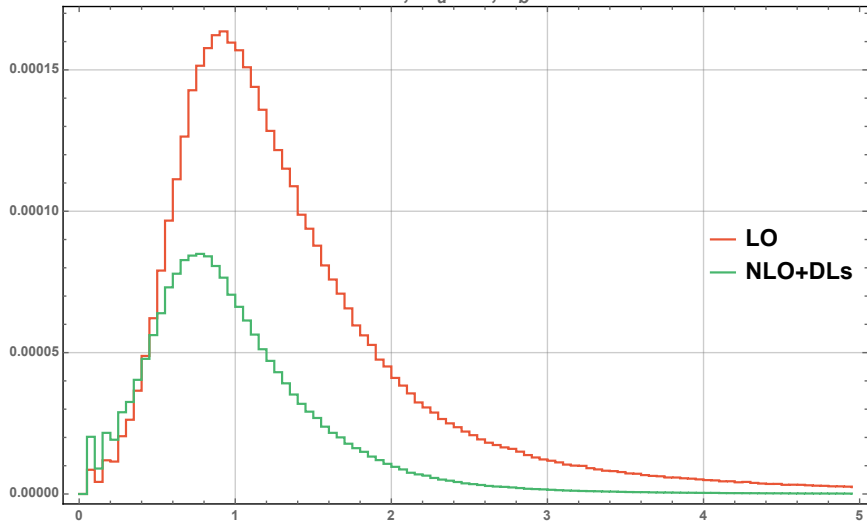
$$y_b(=0) \ll y_n \ll \dots \ll y_2 \ll y_1 \ll y_a$$

$$|k_{b\perp}| \simeq |k_{n\perp}| \simeq \dots \simeq |k_{2\perp}| \simeq |k_{1\perp}| \simeq |k_{a\perp}|$$

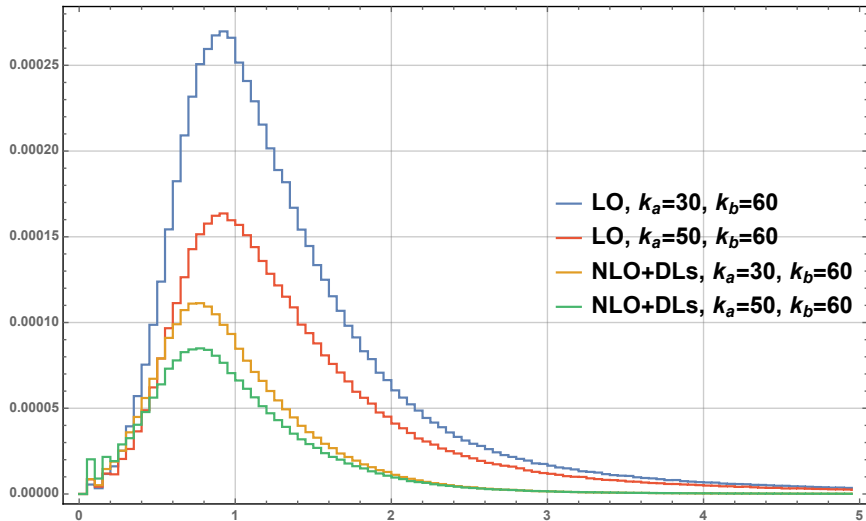
$$\langle \mathcal{R}_{kY} \rangle = \frac{1}{n+1} \sum_{i=1}^{n+1} \frac{k_i e^{y_i}}{k_{i-1} e^{y_{i-1}}}$$

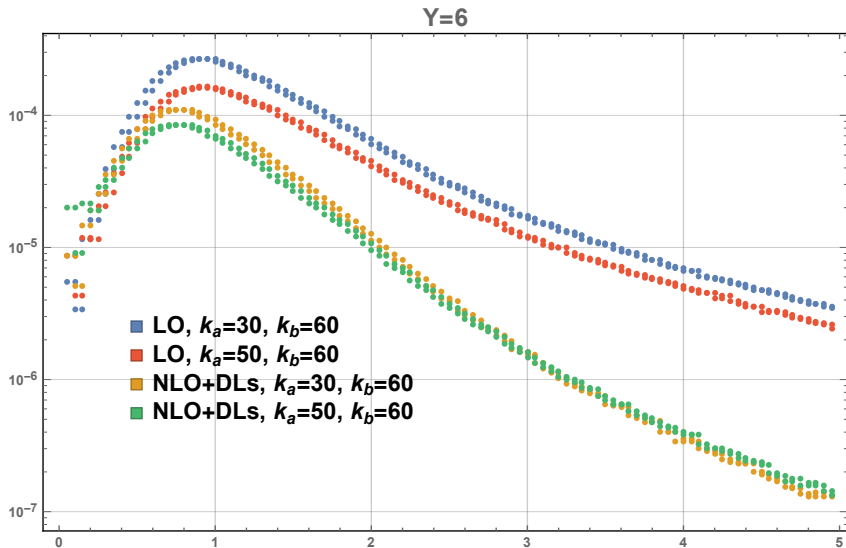
The new observable still probes the rapidity ordering in Multi-Regge kinematics but with the added feature that it also encodes the dependence on the transverse size of the emitted jets.

$Y=6, k_a=30, k_b=60$ 

$Y=6, k_a=50, k_b=60$ 

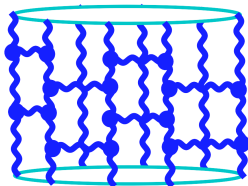
Y=6





- 1 Multi-Regge limit [6]
- 2 Monte Carlo event generator BFKLex [6]
- 3 Collinear double logs [9]
- 4 Odderon & high energy complexity [13]

Amplitudes in the Generalized Leading Logarithmic Approximation (GLLA)



This is an old standing problem in High Energy QCD

Mapped onto a Closed Spin Chain

(Lipatov, Faddeev, Korchemsky,
Janik, Wosiek, Kotanski, Derkachov, Manashov ...)

Monte Carlo integration can be applied in this case (GC-SV)²⁰¹⁶

Let us consider singlet exchange in t -channel with 3 Reggeized gluons:

ODDERON

Degree, Adjacency and Laplacian matrix representations of a graph

Labelled graph	Degree matrix	Adjacency matrix	Laplacian matrix
	$\begin{pmatrix} 2 & 0 & 0 & 0 & 0 & 0 \\ 0 & 3 & 0 & 0 & 0 & 0 \\ 0 & 0 & 2 & 0 & 0 & 0 \\ 0 & 0 & 0 & 3 & 0 & 0 \\ 0 & 0 & 0 & 0 & 3 & 0 \\ 0 & 0 & 0 & 0 & 0 & 1 \end{pmatrix}$	$\begin{pmatrix} 0 & 1 & 0 & 0 & 1 & 0 \\ 1 & 0 & 1 & 0 & 1 & 0 \\ 0 & 1 & 0 & 1 & 0 & 0 \\ 0 & 0 & 1 & 0 & 1 & 1 \\ 1 & 1 & 0 & 1 & 0 & 0 \\ 0 & 0 & 0 & 1 & 0 & 0 \end{pmatrix}$	$\begin{pmatrix} 2 & -1 & 0 & 0 & -1 & 0 \\ -1 & 3 & -1 & 0 & -1 & 0 \\ 0 & -1 & 2 & -1 & 0 & 0 \\ 0 & 0 & -1 & 3 & -1 & -1 \\ -1 & -1 & 0 & -1 & 3 & 0 \\ 0 & 0 & 0 & -1 & 0 & 1 \end{pmatrix}$

Figure from
https://en.wikipedia.org/wiki/Laplacian_matrix

D: Degree matrix
 A: Adjacency matrix
 L: Laplacian matrix
 $L = D - A$

Graph Complexity

The matrix-tree theorem (Kirchhoff, 1847)

A spanning tree T of an undirected graph G is a subgraph that is a tree which includes all of the vertices of G , with minimum possible number of edges.

The complexity of an undirected connected graph corresponds to the number of all possible spanning trees of the graph.

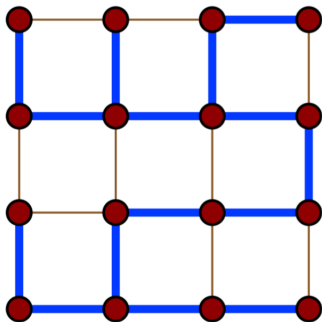
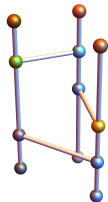


Figure from
https://en.wikipedia.org/wiki/Spanning_tree



Solution of the IR-finite Bartels-Kwiecinski-Praszalowicz (BKP) equation:

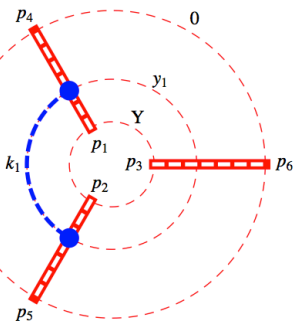
$$\begin{aligned}
 (\omega - \omega(\mathbf{p}_1) - \omega(\mathbf{p}_2) - \omega(\mathbf{p}_3)) f_\omega(\mathbf{p}_1, \mathbf{p}_2, \mathbf{p}_3) = & \\
 \delta^{(2)}(\mathbf{p}_1 - \mathbf{p}_4) \delta^{(2)}(\mathbf{p}_2 - \mathbf{p}_5) \delta^{(2)}(\mathbf{p}_3 - \mathbf{p}_6) & \\
 + \int d^2\mathbf{k} \xi(\mathbf{p}_1, \mathbf{p}_2, \mathbf{p}_3, \mathbf{k}) f_\omega(\mathbf{p}_1 + \mathbf{k}, \mathbf{p}_2 - \mathbf{k}, \mathbf{p}_3) & \\
 + \int d^2\mathbf{k} \xi(\mathbf{p}_2, \mathbf{p}_3, \mathbf{p}_1, \mathbf{k}) f_\omega(\mathbf{p}_1, \mathbf{p}_2 + \mathbf{k}, \mathbf{p}_3 - \mathbf{k}) & \\
 + \int d^2\mathbf{k} \xi(\mathbf{p}_1, \mathbf{p}_3, \mathbf{p}_2, \mathbf{k}) f_\omega(\mathbf{p}_1 + \mathbf{k}, \mathbf{p}_2, \mathbf{p}_3 - \mathbf{k}) &
 \end{aligned}$$



Square of Lipatov's emission vertex:

$$\xi(\mathbf{p}_1, \mathbf{p}_2, \mathbf{p}_3, \mathbf{k}) = \frac{\alpha_s N_c}{4} \frac{\theta(\mathbf{k}^2 - \lambda^2)}{\pi^2 \mathbf{k}^2} \left(1 + \frac{(\mathbf{p}_1 + \mathbf{k})^2 \mathbf{p}_2^2 - (\mathbf{p}_1 + \mathbf{p}_2)^2 \mathbf{k}^2}{\mathbf{p}_1^2 (\mathbf{k} - \mathbf{p}_2)^2} \right)$$

Gluon Regge trajectory: $\omega(\mathbf{p}) = -\frac{\bar{\alpha}_s}{2} \ln \frac{\mathbf{p}^2}{\lambda^2}$

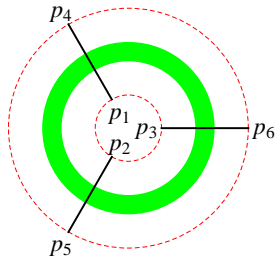


$$\begin{aligned}
 &= \int d^2\mathbf{k}_1 \int_0^Y dy_1 \delta^{(2)}(\mathbf{p}_3 - \mathbf{p}_6) \delta^{(2)}(\mathbf{k}_1 + \mathbf{p}_1 - \mathbf{p}_4) \delta^{(2)}(-\mathbf{k}_1 + \mathbf{p}_2 - \mathbf{p}_5) \\
 &\times \xi(\mathbf{p}_1, \mathbf{p}_2, \mathbf{p}_3, \mathbf{k}_1) e^{\omega(\mathbf{p}_3)Y} e^{(\omega(\mathbf{k}_1 + \mathbf{p}_1) + \omega(\mathbf{p}_2 - \mathbf{k}_1))y_1} e^{(\omega(\mathbf{p}_1) + \omega(\mathbf{p}_2))(Y - y_1)}
 \end{aligned}$$

The interaction builds up rung by rung

We can pick up two configurations with different transferred momentum:

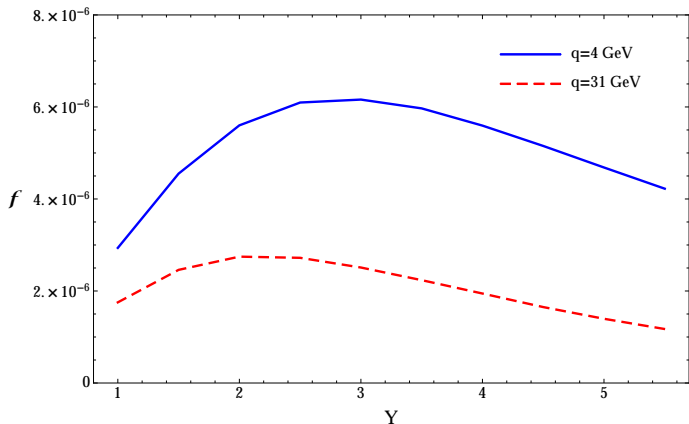
$\mathbf{q} = (4, 0)$	$\mathbf{q} = (31, 0)$
$\mathbf{p}_1 = (10, 0)$	$\mathbf{p}_1 = (10, 0)$
$\mathbf{p}_2 = (20, \pi)$	$\mathbf{p}_2 = (20, \pi)$
$\mathbf{p}_3 = (\mathbf{q} - \mathbf{p}_1) - \mathbf{p}_2 = (14, 0)$	$\mathbf{p}_3 = (\mathbf{q} - \mathbf{p}_1) - \mathbf{p}_2 = (41, 0)$
$\mathbf{p}_4 = (20, 0)$	$\mathbf{p}_4 = (20, 0)$
$\mathbf{p}_5 = (25, \pi)$	$\mathbf{p}_5 = (25, \pi)$
$\mathbf{p}_6 = (\mathbf{q} - \mathbf{p}_4) - \mathbf{p}_5 = (9, 0)$	$\mathbf{p}_6 = (\mathbf{q} - \mathbf{p}_4) - \mathbf{p}_5 = (36, 0)$



and study its growth with energy (GC-SV)²⁰¹⁶.

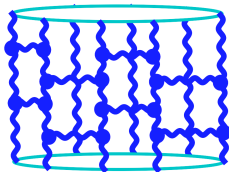
Only the sum of all possible diagrams is IR finite.
We calculate Green functions, not eigenfunctions.

Our solution must contain previous solutions in the literature.
They are singled out by particular impact factors (work in progress).



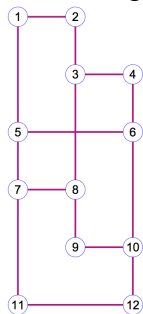
On-going work on phenomenological applications.

Closed Chain with 3 Reggeons (Odderon)



Example, consider the Laplacian matrix L of the diagram with 6 rungs

$$L = \begin{pmatrix} 2 & -1 & 0 & 0 & -1 & 0 & 0 & 0 & 0 & 0 & 0 & 0 & 0 \\ -1 & 2 & -1 & 0 & 0 & 0 & 0 & 0 & 0 & 0 & 0 & 0 & 0 \\ 0 & -1 & 3 & -1 & 0 & 0 & 0 & -1 & 0 & 0 & 0 & 0 & 0 \\ 0 & 0 & -1 & 2 & 0 & -1 & 0 & 0 & 0 & 0 & 0 & 0 & 0 \\ -1 & 0 & 0 & 0 & 3 & -1 & -1 & 0 & 0 & 0 & 0 & 0 & 0 \\ 0 & 0 & 0 & -1 & -1 & 3 & 0 & 0 & 0 & -1 & 0 & 0 & 0 \\ 0 & 0 & 0 & 0 & -1 & 0 & 3 & -1 & 0 & 0 & -1 & 0 & 0 \\ 0 & 0 & -1 & 0 & 0 & 0 & -1 & 3 & -1 & 0 & 0 & 0 & 0 \\ 0 & 0 & 0 & 0 & 0 & 0 & 0 & 0 & -1 & 2 & -1 & 0 & 0 \\ 0 & 0 & 0 & 0 & 0 & -1 & 0 & 0 & -1 & 3 & 0 & -1 & 0 \\ 0 & 0 & 0 & 0 & 0 & 0 & -1 & 0 & 0 & 0 & 2 & -1 & 0 \\ 0 & 0 & 0 & 0 & 0 & 0 & 0 & 0 & 0 & -1 & -1 & 2 & 0 \end{pmatrix}$$

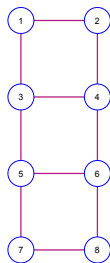


Graph Complexity

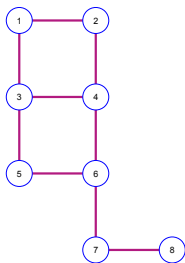
Number of possible spanning trees in a given graph.
(Diagrams crossing all nodes with no loops)

Matrix Tree theorem by Kirchoff:

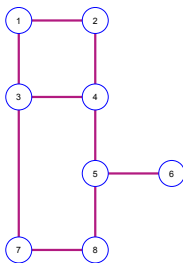
Determinant of any principal minor of L = Complexity of the graph



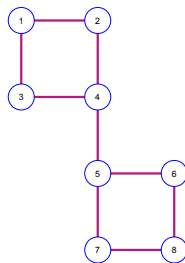
[56]



[15]

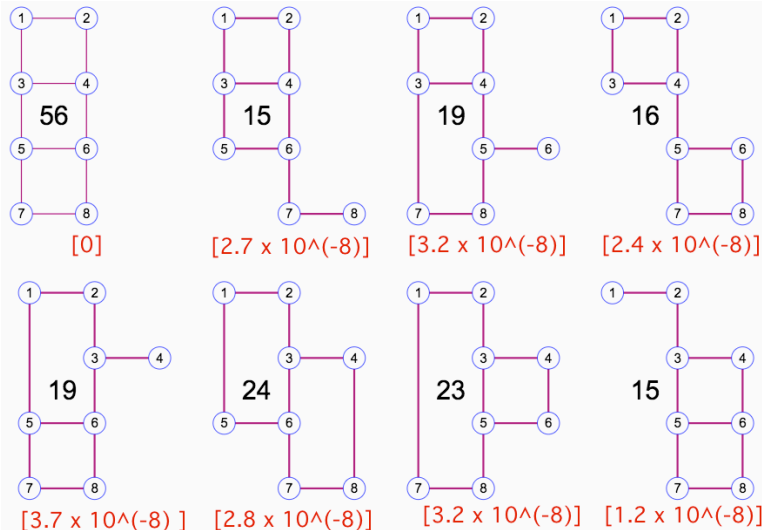


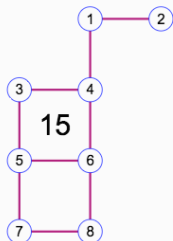
[19]



[16]

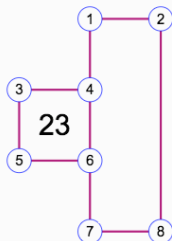
For some external momenta, each graph topology with 4 rungs and associated Graph Complexity contributes to Green function as





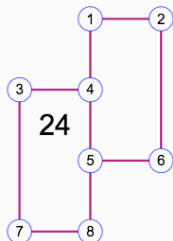
15

$[4.3 \times 10^{(-8)}]$



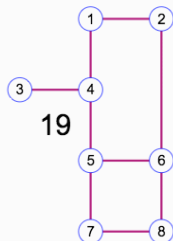
23

$[3.2 \times 10^{(-8)}]$



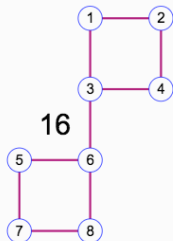
24

$[3.7 \times 10^{(-8)}]$



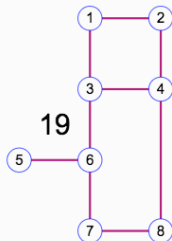
19

$[1.5 \times 10^{(-8)}]$



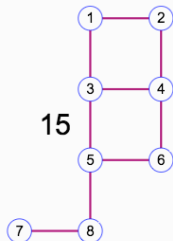
16

$[4.2 \times 10^{(-8)}]$



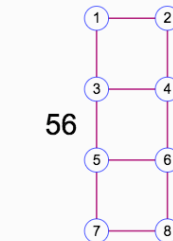
19

$[1.9 \times 10^{(-8)}]$



15

$[2.3 \times 10^{(-8)}]$



56

$[0]$

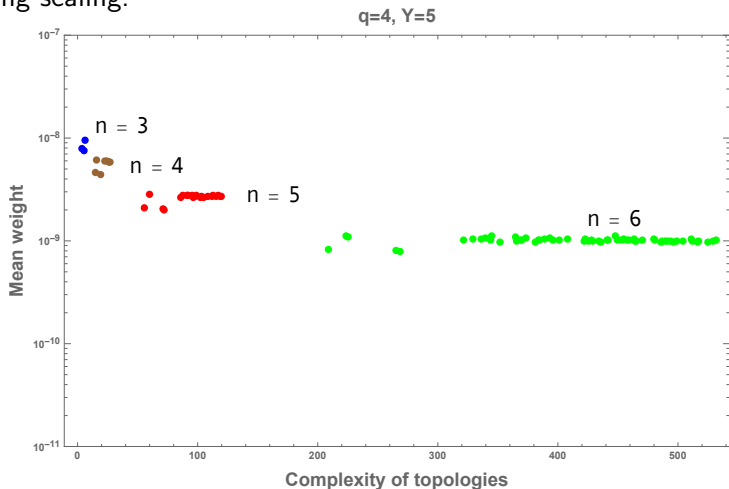
Number of Rungs = 4

We evaluate the average contribution to the GGF per Complexity Class:

Complexity	# diagrams	Average weight in GGF
15	4	2.6×10^{-8}
16	2	3.3×10^{-8}
19	4	2.6×10^{-8}
23	2	3.2×10^{-8}
24	2	3.3×10^{-8}
56	2	0

A “Complexity Democracy” emerges ...

Average weight per complexity class for Reggeon webs.
Emerging scaling.



Due to Lipatov's integrability?

- 1 Multi-Regge limit [6]
- 2 Monte Carlo event generator BFKLex [6]
- 3 Collinear double logs [9]
- 4 Odderon & high energy complexity [13]